

## Reflectance Anisotropy Spectra of the Diamond (100)-(2 × 1) Surface: Evidence of Strongly Bound Surface State Excitons

Maurizia Palummo,<sup>1</sup> Olivia Pulci,<sup>1</sup> Rodolfo Del Sole,<sup>1</sup> Andrea Marini,<sup>2</sup> M. Schwitters,<sup>3</sup> S. R. Haines,<sup>3</sup> K. H. Williams,<sup>3</sup> D. S. Martin,<sup>3</sup> P. Weightman,<sup>3</sup> and J. E. Butler<sup>4</sup>

<sup>1</sup>*Dipartimento di Fisica-Università di Roma, 'Tor Vergata' and Istituto Nazionale per la Fisica della Materia, I-00133 Roma, Italy*

<sup>2</sup>*Departamento da Fisica da Materialas, Facultad de Ciencias Químicas UPV/EHU Centro Mixto CISC-UPV/UHV and Donostia International Physics Center, E-20018 San Sebastian, Basqua Country, Spain*

<sup>3</sup>*Department of Physics, University of Liverpool, Liverpool, L69 3BX, United Kingdom*

<sup>4</sup>*Naval Research Laboratory, Washington, D.C. 20375, USA*

(Received 3 June 2004; published 3 March 2005)

We compare the results of *ab initio* calculations with measured reflection anisotropy spectra and show that strongly bound surface-state excitons occur on the clean diamond (100) surface. These excitons are found to have a binding energy close to 1 eV, the strongest ever observed at a semiconductor surface. Important electron-hole interaction effects on the line shape of the optical transitions above the surface-state gap are also found.

DOI: 10.1103/PhysRevLett.94.087404

PACS numbers: 78.68.+m, 71.35.-y, 73.20.-r, 78.40.-q

Diamond is a material exhibiting extreme physical properties which gives it considerable technological potential. The demonstration of a negative electron affinity [1–3] and a unique surface conductivity among semiconductors is particularly attractive for applications in optoelectronics and electronic devices and has led to the creation of a novel field effect transistor [4]. The realization of diamond's potential in electronic devices is dependent on controlling the physical structure and understanding the electronic structure of its surfaces. The former is difficult due to the metastability and the extreme hardness of the material which makes it difficult to produce atomically flat surfaces via polishing, sputter cleaning, and annealing. The latter is complicated by the uncertainty over the influence of hydrogen on the surface electronic structure [5] and by the need to take into account many-body effects for a correct understanding of experimental results.

Many-body effects show up in band energies as shifts, with respect to one-particle levels, due to the interaction of an electron or hole with the other electrons (self-energy shifts), whose main effect is to increase the gaps between filled and empty states. Moreover, in optical spectra it is crucial to take into account the interaction of the electron and hole generated in the optical transition (excitonic effects) and their screening by the other electrons. Not only the absorption line shape can be modified with respect to independent-particle theory [6], but bound electron-hole states (excitons) can occur below the onset of interband transitions [7,8]. The optical spectra of Si(111)- and Ge(111)-(2 × 1) surfaces [9,10] below 1 eV are currently interpreted in terms of surface-state excitons, with a binding energy of about 0.25 eV [11,12]. Stronger excitonic effects are expected on diamond surfaces due to the smaller dielectric constant. In this Letter we compare the results of *ab initio* calculations with measured reflection anisotropy spectra (RAS). RAS is an optical technique that achieves

surface sensitivity by measuring the difference in reflection from two directions at right angles in a surface of normal incident light, a geometry that leads to a cancellation of the contribution from the bulk of cubic crystals [13,14]. The comparison shows the presence of strongly bound surface-state excitons and important distortions of the RAS line shape above the band gap.

Experimentally we take advantage of recent developments [15] which combine mechanical polishing and chemical and plasma treatments to produce atomically smooth (100) surfaces on a type IIb natural diamond, of dimensions 8 × 2.5 × 4 mm<sup>3</sup> obtained from De Beers. The experiments were performed on a type IIb diamond since its conductivity, which arises from B doping at a level less than a part per million, made it possible to characterize the surface by LEED and x-ray photoelectron spectroscopy (XPS). Similar RAS results would be expected from type IIa diamonds, which are insulators. Vicinal surfaces orientated 4° toward the (110) direction were also produced and the orientations confirmed by x-ray diffraction. The H terminated surfaces were produced in the Naval Research Laboratory in Washington D.C. and transported to Liverpool under ethyl alcohol and then inserted into an ultrahigh vacuum (UHV) chamber. Gentle heating to 500 K in UHV removed adventitious adsorbed hydrocarbon and oxygen species and produced surfaces which showed excellent LEED patterns characteristic of the H/C(100)-(2 × 1) reconstruction [15]. XPS excited by monochromated Al K $\alpha$  x rays showed the single component C 1s photoelectron line shape observed from H terminated surfaces [16]. The diamond was then heated to 1300 K for 30 min to drive off H, and the resultant surface showed a (2 × 1) LEED pattern and a C 1s XPS line shape with a shoulder on the high kinetic energy side, which has been identified with C-C dimers on the C(100)-(2 × 1) reconstructed surface [16]. A subsequent anneal of the 4°

vicinal surface at 1500 K produced an increase in the intensity of the shoulder to high kinetic energy of the C 1s XPS line which showed that the 1300 K anneal does not drive off all the H from the surface or alternatively that some of the H is reabsorbed before it is pumped away. RAS measurements were carried out, using a spectrometer based on the Aspnes design [13], on H terminated flat and 4° vicinal surfaces, and after heat treatment at 1300 K. Scanning tunneling microscopy of the H/C(100) surface in UHV showed the characteristic C-C dimer structure of  $1 \times 2$  and  $2 \times 1$  terraces separated by monatomic steps [17] and the presence of biatomic steps between terraces with the same dimer orientation. Atomic force microscopy in air showed the surfaces to have root mean square roughness of less than 0.1 nm.

The theoretical band-structure and optical spectra were obtained within the state of the art first-principles approaches based on density functional theory (DFT) and the many-body Green function perturbation theory [18,19]. First the relaxed ground state configuration of the C(100) surface was obtained as a symmetric dimer reconstruction, in agreement with existing literature [20]. We solved self-consistently the Kohn-Sham equation within a DFT-LDA (local density approximation) repeated slab scheme [21], using a symmetric slab of 12 atomic and eight vacuum layers and norm-conserving C pseudopotential [22]. The energy bands were calculated through the *GW* approach, which is based on an expansion of the electron self-energy,  $\Sigma$ , in terms of the dynamically screened Coulomb interaction  $W$  [23]. The *GW* method has been shown to give very accurate band structures of bulk and surface semiconductors [24]. In Fig. 1 the resulting theoretical band structure along the high-symmetry directions of the irreducible Brillouin zone (BZ) is compared with the available direct photoemission data [25]. Finally the optical spectra were calculated, going beyond the one-quasiparticle level, by

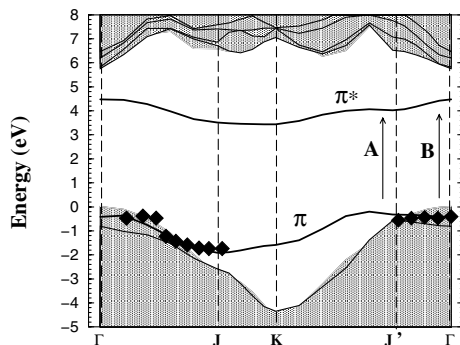


FIG. 1. Electronic band structure of the (100) surface along high-symmetry lines of the  $(2 \times 1)$  BZ including *GW* corrections. The gray regions indicate the projected bulk band structure, while solid lines are the  $\pi$  and  $\pi^*$  dimer surface bands. Arrows A and B mark the transitions which give rise to the two optical structures indicated with the same labels in Fig. 3(b). Experimental data are taken from [25].

including the electron-hole interaction through the solution of the two-particle Green's function Bethe-Salpeter equation. In addition to the electron-hole attractive interaction, the calculation included local-field effects as described in Refs. [6,8,26]. All the details of the calculation will be given elsewhere [27].

Figure 2 shows the RAS measured on the H-covered 4° vicinal surface and on the same surface after annealing at 1300 K. Since the anneal at 1300 K does not remove all the H we expect that, although the measured RAS of this surface will be dominated by the contribution from clean terraces, it will also include contributions from clean steps and H-covered terraces and steps. It has been shown for Si(100) vicinal surfaces that the step contribution cannot be neglected [28], and the different line shapes measured in the present work for 4° C(100) and for 2° (not shown) miscuts confirm this finding. Our calculations for H-covered terraces show that this contribution to the RAS vanishes for frequencies up to 4.8 eV, so that it is not considered here. Calculations also show that clean ideal  $(2 \times 1)$  terraces have vanishing RAS below 2.7 eV, since no electronic transitions occur below this energy. Hence, any observed structure below this energy must be explained in terms of either clean or H-covered steps. The spectra shown in Fig. 2 are almost identical in the range below 2.7 eV, strongly suggesting that the step contribution is the same for the H-covered surface and after annealing at 1300 K. This is not unexpected since it is likely that residual H on the annealed surface resides primarily at the more reactive step sites. Hence, the difference between the two curves in Fig. 2 is proportional to the clean terrace contribution, and this difference is shown in Fig. 3(a). It is important to note that while this difference yields the shape

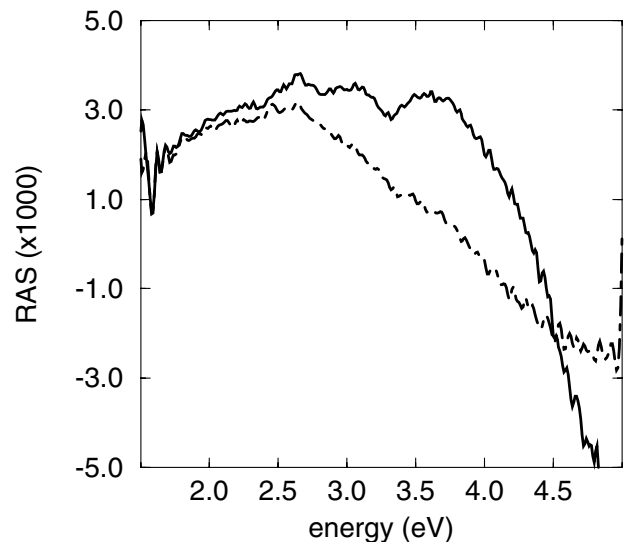


FIG. 2. Experimental RAS for a 4° vicinal surface: clean (solid line) and monohydride (dot-dashed line). The RAS is defined as the relative reflectivity difference between light polarized parallel to the surface dimers and perpendicular to them.

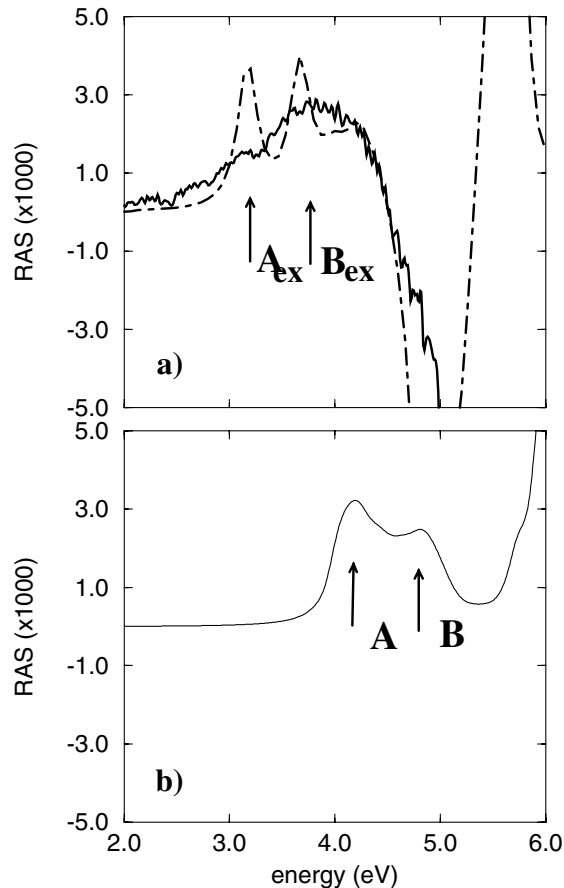


FIG. 3. (a) Theoretical RA spectrum (dot-dashed line), with excitonic, self-energy ( $GW$ ), and local-field effects included, compared with the experimental spectrum (solid line) treated as described in the text. The labels  $A_{ex}$  and  $B_{ex}$  indicate the two bound excitons corresponding to the two one-particle transitions indicated with labels  $A$  and  $B$  in (b). (b) Theoretical RA spectrum with only self-energy ( $GW$ ) and local-field effects included (solid line). RA spectra are defined consistently with Fig. 2.

of the clean terrace contribution to the RAS, it does not yield its absolute intensity which is reduced by the fraction of the terrace area which is still covered by H following the 1300 K anneal. It is further reduced by the presence of domains of oppositely orientated dimers on terraces separated by monatomic steps. The domain balance is almost perfect on the singular C(100) surface as indicated by an almost zero RAS response, while it worsens with an increasing miscut since a large miscut angle favors biatomic steps which preserve the dimer orientation. A reasonable estimate that these effects reduce the RAS intensity by 30% yields good agreement between the measured and calculated absolute RAS intensities [see Fig. 3(a)].

We now draw attention to four features in the RA spectrum (Fig. 2) observed after the 1300 K anneal: the three peaks observed at 2.6, 3.1, and 3.8 eV and the strong dip in the spectrum above 4.5 eV. While a strong reduction

in the intensity of the feature at 2.6 eV is observed in the difference spectrum (solid curve in Fig. 3(a)), indicating that it arises from a step contribution, the features at 3.1 and 3.8 eV are instead only slightly reduced, indicating that they arise from the terraces. Such a slight reduction can be explained by an incomplete H coverage of the surface prior to annealing: in this way, a weak contribution from clean terraces is already present in the dot-dashed spectrum shown in Fig. 2. On the other hand, the negative contribution to the spectrum from 4.0 eV onwards remains strong in the difference spectrum indicating that it is an important feature of the RAS of the clean terraces.

The theoretical RA spectrum shown in Fig. 3(b) was calculated within the independent-quasiparticle (IQP) approximation that includes local-field effects but neglects excitonic effects. Two peaks are clearly apparent, at 4.1 and 4.9 eV. From the surface band structure, shown in Fig. 1, we attribute both peaks to transitions from a filled to an empty surface-state band in the gap. The filled band, just above the valence band, originates from the  $\pi$  bond of the two dangling bonds of a dimer, while the empty surface band, well inside the gap, originates from the  $\pi$  antibond of the same orbitals. Peak  $A$  originates from transitions around  $J'$ , while peak  $B$  originates from transitions at  $\Gamma$  (see Fig. 1). The theoretical RA spectrum of Fig. 3(b), which is consistent with previous one-particle calculations [29], differs from experiments in that the two peaks  $A$  and  $B$  are at too high an energy, and the strong negative contribution from about 4 eV is not reproduced. However, the inclusion of the electron-hole interaction in the calculation has dramatic effects: two strongly bound excitons [ $A_{ex}$  and  $B_{ex}$  in Fig. 3(a)] develop from the corresponding one-particle transitions [ $A$  and  $B$ , in Fig. 3(b)]. The agreement with the experiment is now improved with the main difference being due to the larger broadening of the experimental curve [solid curve, Fig. 3(a)] [30]. The energies of the calculated exciton peaks are in close agreement with the experimental structures at 3.1 and 3.8 eV, which are seen more prominently in the raw data than in the difference spectrum of Fig. 3(a). The importance of the electron-hole interaction can be seen from their effect on the RA spectrum in the region of interband transitions where they completely dominate the spectrum giving rise to the deep negative contribution to the RAS above 4.5 eV. This is determined by the transfer of oscillator strength to lower energies for light polarized parallel to the dimers (due to the formation of bound excitons), with a consequent depletion at higher frequencies.

The calculated binding energy of the two excitons is 0.9 eV, the largest ever found for semiconductors. Surface-state excitons have been found so far for Si(111)- and Ge(111)-(2  $\times$  1) surfaces, with binding energy in both cases close to 0.25 eV [11,12]. Even more striking is the difference with respect to a similar surface, Si(100)-(2  $\times$  1), where the RAS calculated within the IQP approxima-

tion is in qualitative agreement with experiments, suggesting that excitonic effects are weak, with binding energy estimated to be smaller than 0.1 eV [32]. What is the reason for such a large difference between Si and diamond (100) surfaces? The answer is the different surface band structure of the two surfaces: while in the case of C(100) both surface bands are within the gap [as in the case of Si(111)-(2 × 1) and Ge(111)-(2 × 1) surfaces], with the empty one just in the middle of the gap, in the case of Si(100) both surface bands are energetically close to bulk bands. Hence, in the latter case, the mixing of surface bands with bulk bands due to the electron-hole interaction is favored, in such a way that the exciton dynamics is effectively three dimensional. In the case of C(100)-, Si(111)-, and Ge(111)-(2 × 1) surfaces, exciton dynamics is restricted to the dangling bond sites, and is effectively one dimensional: electrons and holes can move along the dimer rows in the first case, and along Pandey's chains in the last two cases. It is well known that the effect of the electron-hole interaction becomes stronger with a decreasing number of dimensions, simply because it is more difficult for electrons and holes to escape their mutual interaction [33]. Finally, the larger binding energy for diamond with respect to Si and Ge(111) can be easily explained in terms of the reduced static screening. In fact, the dielectric constant is about 5 in diamond with respect to 11 in Si. According to a simple effective-mass hydrogenic model of excitons, a factor of 2 in the screening results in a reduction of 4 in the binding energy, very close to our findings.

In conclusion, we have succeeded in preparing high quality diamond (100) surfaces and in measuring the terrace contribution to the RAS. The experimental findings confirm a calculated binding energy of 0.9 eV for the surface-state excitons, the largest ever found in a semiconductor. Strong electron-hole interaction effects on the RAS line shape above the surface states' band gap are found. These effects that we have demonstrated exist on the diamond (100) surface are likely to be important in the design of negative electron affinity devices, the performance of which depends on electrons escaping from the conduction band at the surface, and in attempts to exploit the surface structure of diamond for molecular electronics and biological sensor applications.

This work has been supported by the INFM PAIS project "CELEX," MIUR-COFIN 2002, and by the EU's 6th Framework Programme through the NANOQUANTA Network of Excellence (NMP4-CT-2004-500198). We acknowledge the support of De Beers, the U.K. EPSRC, and CINECA CPU time granted by INFM.

- 
- [1] C. Bandis and B. B. Pate, Phys. Rev. B **52**, 12056 (1995).  
[2] J. Risten, W. Stein, and L. Ley, Phys. Rev. Lett. **78**, 1803 (1997).

- [3] H. J. Looi, R. B. Jackman, and J. S. Foord, Appl. Phys. Lett. **72**, 353 (1998).  
[4] K. Tsugawa *et al.*, Diam. Relat. Mater. **8**, 927 (1999).  
[5] F. Maier *et al.*, Phys. Rev. Lett. **85**, 3472 (2000).  
[6] S. Albrecht, L. Reining, R. Del Sole, and G. Onida, Phys. Rev. Lett. **80**, 4510 (1998).  
[7] M. Rohlfing and S. G. Louie, Phys. Rev. Lett. **80**, 3320 (1998).  
[8] L. X. Benedict, E. L. Shirley, and R. B. Bohn, Phys. Rev. Lett. **80**, 4514 (1998).  
[9] G. Chiarotti *et al.*, Phys. Rev. Lett. **21**, 1170 (1968).  
[10] P. Chiaradia *et al.*, Phys. Rev. Lett. **52**, 1145 (1984).  
[11] M. Rohlfing and S. G. Louie, Phys. Rev. Lett. **83**, 856 (1999).  
[12] M. Rohlfing, M. Palummo, G. Onida, and R. Del Sole, Phys. Rev. Lett. **85**, 5440 (2000).  
[13] D. E. Aspnes, J. P. Harbison, A. A. Studna, and L. T. Florez, J. Vac. Sci. Technol. A **6** 1327 (1988).  
[14] P. Chiaradia and R. Del Sole, Surf. Rev. Lett. **6**, 517 (1999).  
[15] B. D. Thoms, M. S. Owens, J. E. Butler, and C. Spiro, Appl. Phys. Lett. **65**, 2957 (1994).  
[16] J. Wei and J. T. Yates, Crit. Rev. Surf. Chem. **5**, 1 (1995).  
[17] K. Bobrov, A. J. Mayne, and G. Dujardin, Nature (London) **413**, 616 (2001).  
[18] P. Hohenberg and W. Kohn, Phys. Rev. **136**, B864 (1964); W. Kohn and L. J. Sham, Phys. Rev. **140**, A1133 (1965).  
[19] G. Strinati, Riv. Nuovo Cimento **11**, 1 (1988).  
[20] J. Furthmüller, J. Hafner, and G. Kresse, Phys. Rev. B **53**, 7334 (1996).  
[21] D. M. Ceperley and B. J. Alder, Phys. Rev. Lett. **45**, 566 (1980); J. P. Perdew and A. Zunger, Phys. Rev. B **23**, 5048 (1981).  
[22] N. Troullier and J. L. Martins, Phys. Rev. B **43**, 1993 (1991).  
[23] L. Hedin, Phys. Rev. **139**, A796 (1965).  
[24] F. Aryasetiawan and O. Gunnarsson, Rep. Prog. Phys. **61**, 237 (1998), and references therein.  
[25] R. Graupner *et al.*, Phys. Rev. B **57**, 12397 (1998).  
[26] G. Onida, L. Reining, and A. Rubio, Rev. Mod. Phys. **74**, 601 (2002), and references therein.  
[27] M. Palummo *et al.* (to be published).  
[28] S. G. Jaloviar *et al.*, Phys. Rev. Lett. **82**, 791 (1999).  
[29] C. Kress, A. I. Shkrebtii, and R. Del Sole, Surf. Sci. **377-379**, 398 (1997); V. I. Gavrilenko and F. Bechstedt, Phys. Rev. B **56**, 3903 (1997).  
[30] A broadening close to 200 meV is needed in the calculation to reproduce the experimental spectrum. However, the theoretical curve in Fig. 3(a) has been obtained using a smaller broadening  $\gamma = 100$  meV [as at Si(100) [31]] in order to better distinguish the excitonic peaks. The larger experimental broadening at C(100) may be due to several effects, as multiple domains, steps, H-induced disorder, and thermal vibrations.  
[31] M. Palummo *et al.*, Phys. Rev. B **60**, 2522 (1999).  
[32] M. Palummo *et al.* (to be published).  
[33] See R. Loudon, Am. J. Phys. **27**, 649 (1959) for one-dimensional excitons, and M. Shinada and S. Sugano, J. Phys. Soc. Jpn. **21**, 1936 (1966) for two-dimensional excitons.